Protective effects of monosialotetrahexosylganglioside sodium on H_2O_2-induced human vascular endothelial cells

HANG ZHAO[1,2], XIANGJUN LI[1], GUIJIE LI[3], BO SUN[1], LIQUN REN[1] and CONGHAI ZHAO[2]

[1]Department of Experimental Pharmacology and Toxicology, School of Pharmaceutical Science, Jilin University, Changchun, Jilin 130021; Departments of [2]Neurosurgery and [3]Otorhinolaryngology, Head and Neck Surgery, China-Japan Union Hospital of Jilin University, Changchun, Jilin 130033, P.R. China

Received August 21, 2014; Accepted May 14, 2015

DOI: 10.3892/etm.2015.2603

Abstract. Monosialotetrahexosylganglioside sodium (GM1) is widely used in the treatment of central and peripheral neurological injuries. In addition to its neuroprotective activity, GM1 exerts protective effects on brain microvascular endothelial cells, although the mechanisms underlying these effects remain unclear. The aim of the present study was to clarify the protective effects and underlying mechanisms of GM1 on human umbilical vein endothelial cells (HUVECs). In this study, hydrogen peroxide (H_2O_2) was applied to induce the HUVEC injury. HUVECs in a logarithmic growth phase were divided into five groups, namely the control, H_2O_2-treated, 10-mg/l GM1, 5-mg/l GM1 and 1-mg/l GM1 groups. In all the groups, cell proliferation was detected using a Cell Counting Kit-8 assay, a flow cytometric method was applied to analyze the cell cycle and nuclear factor (NF)-κB expression was evaluated using immunofluorescence analysis. In addition, the protein expression levels of NF-κB, phosphatidylinositol 3-kinase (PI3K) and glycogen synthase kinase (GSK)-3 were detected via western blot analysis. The results indicated that GM1 exerted significant protective effects on H_2O_2-injured cells by increasing the ratio of cells in the S/G_2 phase. Furthermore, western blot analysis revealed that PI3K expression levels were markedly increased after 24 h, as a result of the GM1 treatment, while the expression of both GSK-3 markedly decreased. In addition, the ratio of nuclear-to-cytoplasmic NF-κB expression increased in the GM1-treated cells. In summary, GM1 exhibited marked protective effects on the HUVECs, possibly due to the ability of GM1 in maintaining the integrity of the endothelium and increasing the proportion of cells undergoing mitosis, a process in which the PI3K/GSK-3 and NF-κB pathways are crucially involved.

Correspondence to: Dr Liqun Ren, Department of Experimental Pharmacology and Toxicology, School of Pharmaceutical Science, Jilin University, 1266 Fujin Street, Changchun, Jilin 130021, P.R. China
E-mail: renlq@jlu.edu.cn

Dr Conghai Zhao, Department of Neurosurgery, Head and Neck Surgery, China-Japan Union Hospital of Jilin University, 126 Xiantai Street, Changchun, Jilin 130033, P.R. China
E-mail: 187111576@qq.com

Key words: monosialotetrahexosylganglioside, endothelial cells, nuclear factor-κB, phosphatidylinositol 3-kinase, glycogen synthase kinase-3

Introduction

Gangliosides are molecules composed of a glycosphingolipid, consisting of ceramide and oligosaccharides, with one or more sialic acids linked to the sugar chain. The molecules are components of the cell plasma membrane that modulate cell signal transduction events, and have been shown to be concentrated in lipid rafts. Gangliosides have recently been identified as crucial molecules in neuronal apoptosis (1) and endoplasmic reticulum stress response (2). Natural and semisynthetic gangliosides are considered to be possible therapeutics for neurodegenerative disorders (3).

The natural structure of monosialotetrahexosylganglioside (GM1) is galactose-N-acetyl galactosamine-galactose-(glucose-ceramide)-sialic acid (Fig. 1). Semisynthetic gangliosides are sodium salts of GM1, with a molecular formula of $C_{73}H_{130}N_3NaO_{31}$ or $C_{75}H_{134}N_3NaO_{31}$ and a molecular weight of 1,568.84 or 1,597.18 Da, respectively (4). GM1 has been widely used to treat neonatal hypoxic-ischemic brain injury, Parkinson's disease, acute cerebral infarction, retinal ischemia and spinal cord injury (5-7). In addition to neuroprotective effects (8), GM1 has been shown to exert protective effects on brain microvascular endothelial cells (8), although the underlying mechanisms remain unclear.

The phosphatidylinositol 3-kinase (PI3K)/glycogen synthase kinase (GSK)-3 signaling pathway functions primarily as an inhibitory pathway in cells, exerting effects on cell proliferation. Nuclear factor (NF)-κB is a ubiquitous nuclear factor in cells that induces numerous pathological processes, including inflammation, immune cell proliferation and apoptosis. The aim of the present study was to clarify the protective effects and the mechanism of action of GM1 on human umbilical vein endothelial cells (HUVECs).

Materials and methods

Reagents and antibodies. GM1 was supplied by Jilin Yinglian Biopharmaceutical Co., Ltd. (Panshi, China). Dulbecco's modified Eagle's medium (DMEM; SH30021.01) and newborn calf serum (SH30401.01) were obtained from GE Healthcare Life Sciences (HyClone; Logan, UT, USA). A Cell Counting Kit (CCK)-8 was purchased from Guangzhou Yiyuan Biotechnology Co., Ltd. (Guangzhou, China). Mouse monoclonal anti-PI3K p85 (sc-377482), anti-NF-κB p65 (sc-8008) and anti-p-GSK-3 (sc-81496) antibodies were acquired from Santa Cruz Biotechnology, Inc. (Dallas, TX, USA). In addition, a mouse anti-GAPDH monoclonal antibody (TA-08), horseradish peroxidase (HRP)-labeled goat anti-mouse IgG (ZB-2305) and tetramethylrhodamine (TRITC)-conjugated AffiniPure IgG (ZF-0313) were obtained from Beijing Zhongshan Golden Bridge Biotechnology Co., Ltd. (Beijing, China). An enhanced chemiluminescence (ECL) detection kit (NCI5079) was purchased from EMD Millipore (Billerica, MA, USA). Furthermore, a Bradford protein assay kit (P0006), radioimmunoprecipitation assay (RIPA) lysis buffer (P0013B) and a nuclear and cytosolic protein extraction kit (P0027) were acquired from the Beyotime Institute of Biotechnology (Guangzhou, China).

Cell culture and grouping. HUVECs were purchased from Shanghai Bogoo Biotechnology Co., Ltd. (Shanghai, China). The HUVEC strain was cultured and passaged routinely in DMEM culture medium containing 10% fetal bovine serum in 5% CO_2 at 37˚C. Subsequently, the cells were divided into five groups. Only serum-free DMEM was used in the control group. H_2O_2 was used to induce lesions in the HUVECS. The H_2O_2-treated cells (H_2O_2 group) were cultured with 500 mmol/l H_2O_2 in serum-free DMEM, while the cells in the high-dose GM1 group (10-mg/l GM1; GM1 H group) were cultured in serum-free DMEM with 500 mmol/l H_2O_2 containing 10 mg/l GM1. In addition, the medium-dose GM1 group cells (5-mg/l GM1; GM1 M group) were cultured in serum-free DMEM with 500 mmol/l H_2O_2 containing 5 mg/l GM1, and the low-dose GM1 group cells (1-mg/l GM1; GM1 L group) were cultured in serum-free DMEM with 500 mmol/l H_2O_2 containing 1 mg/l GM1. All the cells were cultured in serum-free DMEM for 12 h, which was exchanged for the conditional medium, as aforementioned, in order to synchronize the cells.

Detection of cell proliferation. Cell proliferation was detected using a CCK-8 assay. HUVECs were plated in 96-well plates at a density of ~$1x10^3$ cells per well. Following treatment under the different culture medium conditions for 24 h, 10 μl CCK-8 was added and the plates were cultured for an additional 2 h, and the optical density value at 490 nm was determined using a DNM-9606 plate reader (Beijing Perlong Medical Equipment Co., Ltd., Beijing, China). The cell viability was calculated according to the following formula: Cell viability (%) = (treated group - control group) x 100%. The experiment was repeated three times, using a minimum of six wells for each group each time.

Cell cycle analysis. Flow cytometry (FCM) was applied to analyze the cell cycle. HUVECs in a logarithmic growth phase were seeded in six-well plates at a density of $5x10^5$ cells per well. Following treatment under the different culture medium conditions for 24 h, the culture medium was discarded and the cells were collected via routine trypsin digestion. Next, the cells were incubated overnight with 1 ml alcohol (70%) at 4˚C. Following centrifugation at 300 x g for 5 min, the alcohol was discarded and the pellet was washed three times with pre-chilled phosphate-buffered saline (PBS) buffer. Finally, the cells were stained with 50 μm/ml propidium iodide for 30 min at 4˚C and the cell cycle ratio was evaluated using a FACSCalibur cell analyzer (BD Biosciences, Franklin Lakes, NJ, USA). At least 3 wells had been used for each group and the all experiments were repeated 3 times.

Immunofluorescence assay. Briefly, cells in a logarithmic phase were seeded into 24-well plates at a density of $5x10^3$ cells per well. After 24 h, following cell adhesion to the sides of the well, the conditional medium was exchanged as aforementioned. The slides were treated with 4% paraformaldehyde solution for 30 min, washed three times in 0.01 mol/l PBS (pH 7.4) and placed in goat non-immune serum (ZDR-5117; Beijing Zhongshan Golden Bridge Biotechnology Co., Ltd., Beijing, China) for 20 min at room temperature. Next, the slides were transferred to an NF-κB p65 monoclonal antibody solution (1:200) and incubated overnight at 4˚C. The slides were subsequently washed three times, as aforementioned, and buffer containing TRITC-conjugated AffiniPure goat anti-mouse IgG (1:1,000) was added to the slides, followed by incubation for 1 h at room temperature. Finally, the slides were sealed with glycerol and photographed using a Nikon 80i fluorescence microscope (Nikon Corporation, Tokyo, Japan).

Total protein detection. Total protein content in each sample was determined using the Bradford method. According to the manufacturer's instructions of the Bradford protein assay kit, 5 μl cell lysis buffer was diluted to 20 μl in standard dilution buffer, followed by mixing with 200 μl G-250 solution in a 96-well plate and incubation for 3-5 min at room temperature. A standard curve was generated using bovine serum albumin (BSA; A4503; Sigma-Aldrich, St. Louis, MO, USA) as a reference. The absorbance was measured at 490 nm, and the resulting values were referenced with the standard curve to calculate the protein concentration in the samples.

Western blot analysis. For the measurement of PI3K and p-GSK3 protein expression levels, the cells were incubated for 3-5 min at room temperature, after which the protein was extracted using ice-cold RIPA buffer containing 2 μg/ml leupeptin, 2 μg/ml aprotinin, from the previously mentioned RIPA and cytosolic protein extraction kits, respectively, and 100 μg/ml phenylmethylsulfonyl fluoride (IPFL00010; EMD Millipore). Protein concentrations were determined using a Bradford method assay, as aforementioned. Subsequently, ~15-mg samples of whole-cell lysate protein were added to each lane and resolved using 10% SDS-PAGE, after which the protein was transferred to a 0.22-μM polyvinylidene fluoride membrane. Non-specific biding sites on the membrane were blocked with BSA for 1 h at room temperature. Next, the membranes were incubated with the mouse monoclonal PI3K (1:200) and p-GSK3α/β (1:200) primary antibodies overnight

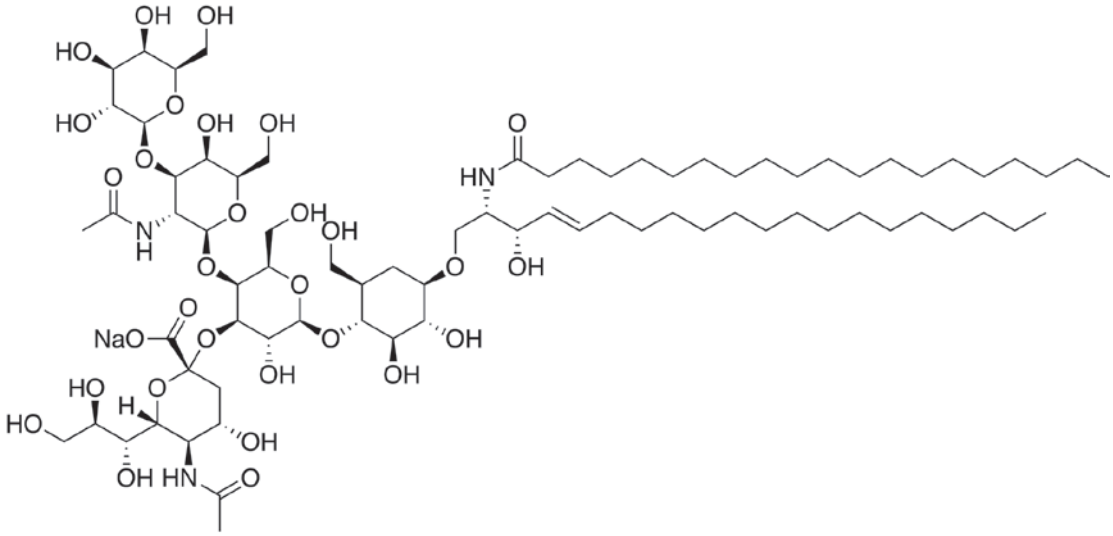

Figure 1. Structure of monosialotetrahexosylganglioside sodium.

at 4˚C. GAPDH (1:1,000) was used as an internal control, and the HRP-conjugated goat anti-mouse IgG (1:2,000; 1 h at room temperature) was used as the secondary antibody. The resultant signals were detected using ECL analysis, and ImageJ software, version 1.46 (National Institutes of Health, Bethesda, MD, USA) was employed to quantify the band densities. The band densities of PI3K and p-GSK3α/β were normalized against that of GAPDH throughout the experiment, which was used as the final measure of expression.

NF-κB p65 expression assay. NF-κB p65 expression levels in the cytoplasm and nucleus were assessed using western blot analysis. Firstly, total nuclear and cytoplasmic protein was isolated using a protein extraction kit. According to the manufacturer's instructions, the cells were collected via scraping and lysed in cytoplasm extraction solution. Following centrifugation at 12,000-16,000 x g for 5 min at 4˚C. The supernatant which containing cytoplasm protein was retained, and nuclear extraction solution was added to the precipitate in order to extract nuclear protein. Nuclear and the cytoplasmic protein were analyzed using western blot analysis as previously described.

Statistical analysis. All the experiments were independently replicated a minimum of three times. The obtained data are expressed as the mean ± standard deviation, and the results were evaluated via one-way analysis of variance using GraphPad Prism software, version 5 (GraphPad Software, Inc., La Jolla, CA, USA). P<0.05 was considered to indicate a statistically significant difference.

Results

Protective proliferation-inducing effects of GM1 on H_2O_2-induced HUVEC lesions. Results of the CCK-8 assay indicated that the cell survival rate in the H_2O_2-treated group was 75.97% (79.97±11.77%), which was significantly reduced compared with the control group (100%; Fig. 2A). In addition, when compared with the H_2O_2-treated group, the cell survival rates in the 10 and 5-mg/l GM1-treated groups were significantly reduced (P<0.001 and P<0.05, respectively), whereas the difference in the cell survival rate between the 1-mg/l GM1-treated group and the control group was not statistically significant. Fig. 2B and C shows the FCM data used for cell cycle analysis to quantify the ratio of cells in the G_2 and S phase in the various experimental groups. In the control group, 50.87±4.29% of the total cells were in the G2 and S phases, while in the H_2O_2-treated group, only 13.52% of the total cells were in the G2 and S phases, indicating a significant difference between the two groups (P<0.001). In the GM1-treated groups, the ratio of cells in the G_2 and S phases was significantly increased when compared with the H_2O_2-treated group (P<0.001; Fig. 2C).

Effects of GM1 on PI3K and GSK3α/β expression levels in H_2O_2-induced HUVEC lesions. Changes in the protein expression levels of PI3K and GSK3α/β in the H_2O_2-induced HUVEC lesions with or without the protective effects of GM1 were assessed using western blot analysis (Fig. 3). Densitometric analysis revealed significantly lower expression levels of PI3K in the H_2O_2-treated group when compared with the control group (P<0.01). Furthermore, PI3K expression levels were significantly increased in the 10 and 5-mg/l GM1-treated groups when compared with the H_2O_2-treated group (P<0.01 and P<0.05, respectively).

With regard to GSK-3 expression, one band at 51 kDa corresponded to p-GSK-3α, and the second band at 47 kDa corresponded to p-GSK-3β. Densitometric analysis revealed that p-GSK-3 expression levels in the H_2O_2-treated cells were significantly increased compared with the control group (P<0.01). In the GM1-treated groups, the p-GSK-3α/β expression levels were decreased when compared with the H_2O_2-treated group, and the differences were statistically significant (P<0.05).

Effects of GM1 on NF-κB expression in HUVECs. Observations from the indirect immunofluorescence analysis revealed that NF-κB p65 was expressed predominantly in the cytoplasm

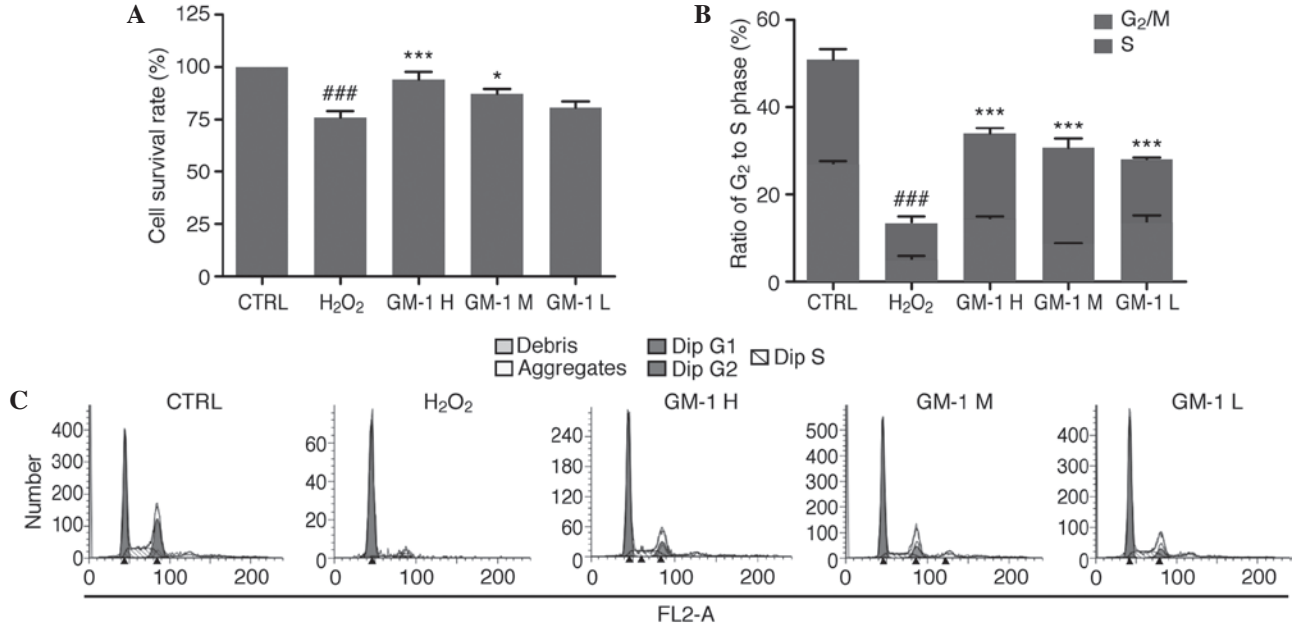

Figure 2. Protective effects of GM1 on H_2O_2-induced human umbilical vein endothelial cell (HUVEC) lesions. (A) Cell survival rate of the HUVECs in the H_2O_2-treated group was significantly decreased compared with the control group, while treatment with high and medium concentrations of GM1 significantly increased the cell survival rate compared with the H_2O_2-treated group. (B) Ratio of cells in the G2 and S phases in the experimental groups. Compared with the control group, the H_2O_2-treated group exhibited a significantly decreased ratio. Compared with the H_2O_2-treated group, all GM1-treated groups exhibited significantly increased ratios. (C) Cell cycle of HUVECs in the various groups analyzed by flow cytometry. $^{\#\#\#}$P<0.00, vs. control group; *P<0.05, **P<0.01 and ***P<0.001 vs. H_2O_2-treated group. CTRL, control; GM1, monosialotetrahexosylganglioside; H, high dose; M, medium dose; L, low dose.

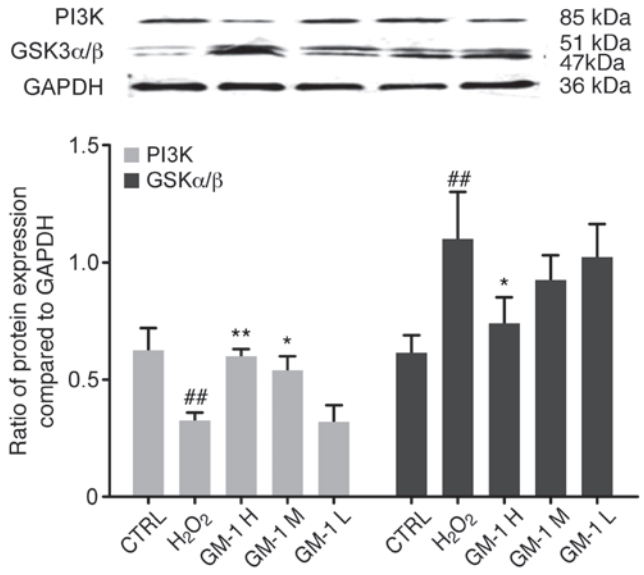

Figure 3. PI3K and GSK-3 protein expression levels were determined by western blot analysis. When compared with the control group, PI3K expression in the H_2O_2-treated group was decreased significantly. When compared with the H_2O_2-treated group, the high and medium concentrations of GM1 significantly increased PI3K expression levels. Compared with the control group, GSK3α/β expression in the H_2O_2-treated group was increased significantly. When compared with the H_2O_2-treated group, the highest concentration of GM1 significantly decreased GSK3α expression levels. $^{\#\#}$P<0.01, vs. control group; *P<0.05 and **P<0.01, vs. H_2O_2-treated group. CTRL, control; GM1, monosialotetrahexosylganglioside; H, high dose; M, medium dose; L, low dose; PI3K, phosphatidylinositol 3-kinase; GSK, glycogen synthase kinase.

of the cells from the H_2O_2 group, with reduced levels of expression observed in the nucleus (Fig. 4). In the control and GM1-treated groups, the cytoplasm and the nucleus exhibited NF-κB p65 expression. When compared with the H_2O_2 treatment group, nuclear NF-κB p65 expression levels in the 10 and 5-mg/l GM1 treatment groups were significantly increased (P<0.05).

In the western blot assays, NF-κB p65 appeared as a band with a molecular weight of 65 kDa. No statistically significant differences were detected between the experimental groups with regard to the cytoplasmic NF-κB p65 expression levels. Comparison of the nuclear-to-cytoplasmic ratio of NF-κB p65 expression revealed a statistically significant reduction in the H_2O_2-treated group when compared with the control group. The nuclear-to-cytoplasmic ratios of NF-κB p65 in the 10 and 5-mg/l GM1-treated groups were significantly increased compared with the H_2O_2-treated group (P<0.01).

Discussion

Vascular endothelial cell injury is a crucial factor in the pathogenesis of a variety of vascular lesions, and protecting endothelial function is vital for the prevention and treatment of vascular disease (9). H_2O_2 is a common reactive oxygen species that promotes free radical generation, which is able to enter and accumulate within cells, resulting in cellular damage (10). The reported concentrations of H_2O_2 required to induce cell lesions varies widely in the literature (11-13). In the present study, 500 mmol/l H_2O_2 was used, and the results showed that ~10% of the cells were in the DNA synthesis (S) or mitotic (G_2) phase of the cell cycle. In addition, the cell survival rate was ~75% of that observed in the control cells. These data indicate that the proliferation of the HUVECs was inhibited within 24 h of 500 mmol/l H_2O_2 treatment. Although GM1 is hypothesized to function as a neuroprotective agent,

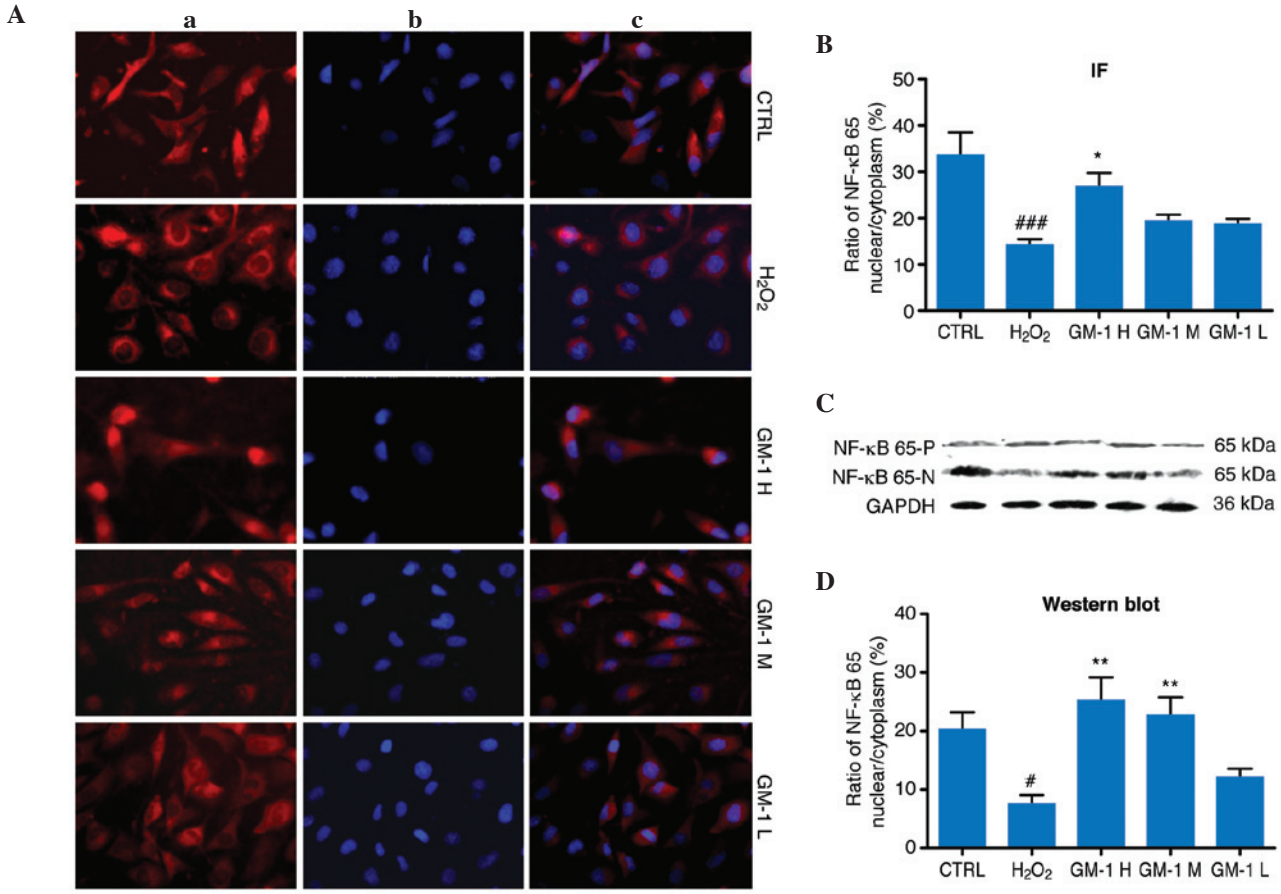

Figure 4. Effects of GM1 on NF-κB expression in human umbilical vein endothelial cells (HUVECs). (A) Examples of the immunofluorescence microscopy images from the various groups: (a) NF-κB positive signals are shown as red; (b) nuclei are stained blue with DAPI; (c) composition of the NF-κB and nuclear staining. (B) Nuclear-to-cytoplasmic ratio of NF-κB of the immunofluorescence in various groups. Compared with the control group, the nuclear-to-cytoplasm ratio of NF-κB in the H_2O_2-treated group decreased significantly (P<0.001), while that in the GM1 H group is markedly increased compared with the H_2O_2-treated group (P<0.05). (C) Representative of NF-κB expression in the nucleus (NF-κB-N) and cytoplasm (NF-κB-P) of the various groups. GAPDH was used as a positive control against NF-κB expression in the cytoplasm. (D) Nuclear-to-cytoplasmic ratio of NF-κB of western blot analysis in various groups. The nuclear-to-cytoplasmic ratio of NF-κB is decreased in the H_2O_2-treated group compared with the control group (P<0.05); while that in the GM1 H and GM1 M groups were increased markedly compared with the H_2O_2-treated group (P<0.05). $^{\#}$P<0.05 and $^{\#\#\#}$P<0.001 vs. control group; *P<0.05 and **P<0.01 vs. H_2O_2-treated group. CTRL, the control group; H_2O_2, H_2O_2-treated group; GM1, monosialotetrahexosylganglioside sodium; H, high dose; M, medium dose; L, low dose; NF, nuclear factor; IF, immunofluorescence.

the molecule exhibited a significant protective effect on H_2O_2-injured cells. The number of cells in the S and G_2 phases increased to ~35% in the GM1 H group, which was almost twice the rate observed in the H_2O_2-treated group. Although the mechanism underlying this observation remains unclear, the outcome may be the result of the similarity between the structures of GM1 and phosphatidylserine, which contributes to cell entry and the maintenance of cell membrane integrity.

PI3K is a lipid kinase that catalyzes the phosphorylation of phosphatidylinositol at the D3 position to yield phosphatidylinositol (3,4,5)-triphosphate (PIP_3). PIP_3 is a secondary messenger that transmits extracellular signals to target proteins downstream of PI3K, inducing numerous biological effects, including cell proliferation, apoptosis and differentiation (14,15). PI3K is composed of the p85 and p110 subunits; p85 lacks PI3K activity and functions as an adapter, coupling p110 to an activated protein tyrosine kinase. PI3K may be activated by numerous extracellular signals that act via receptor tyrosine kinases or G protein-coupled receptors, including growth factors, cytokines and hormones (16). In the present study, western blot analysis was applied to detect the protein expression of PI3K in HUVECs cultured in DMEM, containing 500 mmol/l H_2O_2, with or without GM1 treatment. After 24 h, PI3K expression levels were markedly increased in the GM1-treated cells, indicating that PI3K may be involved in the protective effects of GM1 on H_2O_2-treated cells.

GSK-3 is a multifunctional serine/threonine protein kinase that is hypothesized to be one of the primary target kinases downstream of the PI3K signaling pathway. The majority of studies support the hypothesis that GSK-3 is a key enzyme involved in the regulation of a variety of cellular functions, although the enzyme was initially identified as the rate-limiting enzyme in glycogen metabolism (17). GSK-3 is able to phosphorylate numerous proteins, including transcription factors; thus, the enzyme is involved in the regulation of various cellular functions, including sugar metabolism, the regulation of gene expression and the maintenance of cytoskeletal integrity, and GSK-3 is particularly associated with apoptosis (18). The kinase activity of GSK-3 is controlled via differential phosphorylation of the regulatory serine/threonine residues, which exert an inhibitory effect, and the regulatory tyrosine residues, which exhibit an activating effect. There are

two key forms of GSK-3: GSK-3α and GSK-3β. The activity is controlled via the differential phosphorylation of its regulatory serine/threonine residues, which has an transcription factors that are responsible for coordinating processes, such as glycogen synthesis and cell adhesion (19). Growth factor stimulation of mammalian cells expressing GSK-3α and GSK-3β induces the phosphorylation of Ser 21 and Ser 9, respectively, via the PI3K-dependent pathway, which subsequently enhances proliferative signals. Additionally, GSK-3 physically associates with cAMP-dependent protein kinase A (PKA) (20), which phosphorylates Ser 21 of GSK-3α or Ser 9 of GSK-3β, thereby inactivating the two forms of GSK-3. GSK-3α and GSK-3β are positively regulated by the phosphorylation of Tyr 279 and Tyr 216, respectively. Activated GSK-3 participates in energy metabolism, neuronal cell development and body pattern formation. Tyrosine dephosphorylation of GSK-3 is involved in the extracellular signal-dependent inactivation of the kinase (21). In the present study, GSK-3α and GSK-3β were expressed at markedly higher levels following H_2O_2 treatment, while GM1 treatment decreased the expression levels of these proteins. These results indicate that the protective effects of GM1 on the proliferation of damaged HUVECs may involve the mitigation of GSK-3 overexpression.

NF-κB is a nuclear transcription factor that regulates the expression of a large number of genes, which are critical for the regulation of apoptosis, viral replication, tumorigenesis, inflammation and various autoimmune diseases. NF-κB consists of two subunits, p50 and p65, which are considered to be involved in a stress response, since they are activated by a variety of stimuli, including growth factors, cytokines, lymphokines, ultraviolet radiation, pharmacological agents and stress. If sequestered in the cytoplasm, NF-κB exists in the form of a dimer comprised of the NF-κB p50 and p65 subunits, and the dimer interacts with an inhibitor of κB (IκB), which prevents NF-κB from exhibiting biological activity. The various stimuli that activate NF-κB induce the phosphorylation of IκB, which is followed by its ubiquitination and subsequent degradation. In the nucleus, NF-κB binds to a consensus nucleotide sequence (5'-GGGACTTTC C-3') within the promoters of various genes, subsequently activating their transcription (22). The DNA-binding activity of NF-κB is initiated, followed by rapid transport from the cytoplasm to the nucleus in cells exposed to mitogens or growth factors (23). cDNAs encoding precursors of two distinct proteins have been described and designated as p105 and p100. In cerebral ischemia-reperfusion injury, NF-κB activation is considered to be a key mediator in the process of inflammation and the cascade reaction following ischemia (24). Nurmi *et al* (25) observed that after 24 h of cerebral ischemia-reperfusion injury in rats, the activity of NF-κB was increased by ~260% in the ischemic focus and surrounding areas. In the present study, based on the obtained immunofluorescence results, NF-κB p65 was shown to be predominantly expressed in the cytoplasm, exhibiting reduced expression in the nucleus of the cells exposed to H_2O_2. This observation demonstrates that H_2O_2 treatment may induce a resting state in the majority of HUVECs, in which H_2O_2 inhibits HUVEC proliferation by blocking NF-κB p65 translocation into the nucleus. Separate analysis of NF-κB p65 expression in the cytoplasm and nucleus using western blot analysis revealed that the nuclear-to-cytoplasmic ratio of NF-κB p65 expression was ~10%, which is half the ratio observed in the control cells. When GM1 was administered, the nuclear-to-cytoplasmic ratio of NF-κB p65 expression increased significantly, indicating that increased quantities of NF-κB p65 had entered the nucleus as a result of the treatment. As aforementioned, increased rates of NF-κB p65 translocation into the nucleus result in enhanced rates of transcription. Since NF-κB translocates into the cytoplasm of resting cells and its activation does not require other newly transcribed proteins as mediators, NF-κB is considered to be a rapid reaction switch, enabling the regulation of early gene expression in response to various stimuli.

In conclusion, GM1 was demonstrated to exert marked protective effects on the endothelium, which indicates the novel application of GM1 for the treatment of brain injury. GM1 is able to maintain the integrity of the endothelium and increase cell mitosis, a process in which the PI3K/GSK-3 and NF-κB pathways are crucially involved.

Acknowledgements

This study was supported by a Jilin province Department of Health and Family Commission Foundation fellowship (no. 20140414041GH) and a basic scientific research grant of Jilin University of Jilin University. The authors thank Drs. Yu Xiaoyan and Shi Yan for the assessment of pathological slides.

References

1. Tessitore A, del P Martin M, Sano R, Ma Y, Mann L, Ingrassia A, Laywell ED, Steindler DA, Hendershot LM and d'Azzo A: GM1-ganglioside-mediated activation of the unfolded protein response causes neuronal death in a neurodegenerative gangliosidosis. Mol Cell 15: 753-766, 2004.
2. d'Azzo A, Tessitore A and Sano R: Gangliosides as apoptotic signals in ER stress response. Cell Death Differ 13: 404-414, 2006.
3. Mocchetti I: Exogenous gangliosides, neuronal plasticity and repair and the neurotrophins. Cell Mol Life Sci 62: 2283-2294, 2005.
4. Schwarzmann G, Hofmann P and Pütz U: Synthesis of ganglioside GM1 containing a thioglycosidic bond to its labeled ceramide(s). A facile synthesis starting from natural gangliosides. Carbohydr Res 304: 43-52, 1997.
5. Zhang GZ and Li XG: Cerebral trauma, *Campylobacter jejuni* infection, and monosialotetrahexosylganglioside sodium mediated Guillain-Barré syndrome in a Chinese patient: A rare case event. J Neuropsychiatry Clin Neurosci 26: E16-E17, 2014.
6. Hawryluk GW, Rowland J, Kwon BK and Fehlings MG: Protection and repair of the injured spinal cord: A review of completed, ongoing and planned clinical trials for acute spinal cord injury. Neurosurg Focus 25: E14, 2008.
7. Masson E, Wiernsperger N, Lagarde M and El Bawab S: Involvement of gangliosides in glucosamine-induced proliferation decrease of retinal pericytes. Glycobiology 15: 585-591, 2005.
8. Frontczak-Baniewicz M, Gadamski R, Barskov I and Gajkowska B: Beneficial effects of GM1 ganglioside on photochemically-induced microvascular injury in cerebral cortex and hypophysis in rat. Exp Toxicol Pathol 52: 111-118, 2000.
9. Suzuki Y, Nagai N and Umemura K: Novel situations of endothelial injury in stroke - mechanisms of stroke and strategy of drug development: Intracranial bleeding associated with the treatment of ischemic stroke: Thrombolytic treatment of ischemia-affected endothelial cells with tissue-type plasminogen activator. J Pharmacol Sci 116: 25-29, 2011.
10. Touyz RM and Schiffrin EL: Reactive oxygen species in vascular biology: Implications in hypertension. Histochem Cell Biol 122: 339-352, 2004.

11. Liu L, Gu L, Ma Q, Zhu D and Huang X: Resveratrol attenuates hydrogen peroxide-induced apoptosis in human umbilical vein endothelial cells. Eur Rev Med Pharmacol Sci 17: 88-94, 2013.
12. Suo R, Zhao ZZ, Tang ZH, Ren Z, Liu X, Liu LS, Wang Z, Tang CK, Wei DH and Jiang ZS: Hydrogen sulfide prevents H_2O_2-induced senescence in human umbilical vein endothelial cells through SIRT1 activation. Mol Med Rep 7: 1865-1870, 2013.
13. Liu DH, Chen YM, Liu Y, Hao BS, Zhou B, Wu L, Wang M, Chen L, Wu WK and Qian XX: Ginsenoside Rb1 reverses H_2O_2-induced senescence in human umbilical endothelial cells: Involvement of eNOS pathway. J Cardiovasc Pharmacol 59: 222-230, 2012.
14. Hong SW, Jung KH, Lee HS, Choi MJ, Son MK, Zheng HM and Hong SS: SB365 inhibits angiogenesis and induces apoptosis of hepatocellular carcinoma through modulation of PI3K/Akt/mTOR signaling pathway. Cancer Sci 103: 1929-1937, 2012.
15. Shi F, Wang YC, Zhao TZ, Zhang S, Du TY, Yang CB, Li YH and Sun XQ: Effects of simulated microgravity on human umbilical vein endothelial cell angiogenesis and role of the PI3K-Akt-eNOS signal pathway. PLoS One 7: e40365, 2012.
16. Lu C, Ha T, Wang X, Liu L, Zhang X, Kimbrough EO, Sha Z, Guan M, Schweitzer J, Kalbfleisch J, Williams D and Li C: The TLR9 ligand, CpG-ODN, induces protection against cerebral ischemia/reperfusion injury via activation of PI3K/Akt signaling. J Am Heart Assoc 3: e000629, 2014.
17. Li X, Zhang J, Chai S and Wang X: Progesterone alleviates hypoxic-ischemic brain injury via the Akt/GSK-3β signaling pathway. Exp Ther Med 8: 1241-1246, 2014.
18. Choi SE, Kang Y, Jang HJ, Shin HC, Kim HE, Kim HS, Kim HJ, Kim DJ and Lee KW: Involvement of glycogen synthase kinase-3beta in palmitate-induced human umbilical vein endothelial cell apoptosis. J Vasc Res 44: 365-374, 2007.
19. Doble BW and Woodgett JR: Role of glycogen synthase kinase-3 in cell fate and epithelial-mesenchymal transitions. Cells Tissues Organs 185: 73-84, 2007.
20. Wu HM, Lee CG, Hwang SJ and Kim SG: Mitigation of carbon tetrachloride-induced hepatic injury by methylene blue, a repurposed drug, is mediated by dual inhibition of GSK3β downstream of PKA. Br J Pharmacol 171: 2790-2802, 2014.
21. Eigler T, Ben-Shlomo A, Zhou C, Khalafi R, Ren SG and Melmed S: Constitutive somatostatin receptor subtype-3 signaling suppresses growth hormone synthesis. Mol Endocrinol 28: 554-564, 2014.
22. Kim JM, Lee EK, Park G, Kim MK, Yokozawa T, Yu BP and Chung HY: Morin modulates the oxidative stress-induced NF-kappaB pathway through its anti-oxidant activity. Free Radic Res 44: 454-61, 2010.
23. Urban MB and Baeuerle PA: The role of the p50 and p65 subunits of NF-kappaB in the recognition of cognate sequences. New Biol 3: 279-288, 1991.
24. Howard EF, Chen Q, Cheng C, Carroll JE and Hess D: NF-kappa B is activated and ICAM-1 gene expression is upregulated during reoxygenation of human brain endothelial cells. Neurosci Lett 248: 199-203, 1998.
25. Nurmi A, Lindsberg PJ, Koistinaho M, Zhang W, Juettler E, Karjalainen-Lindsberg ML, Weih F, Frank N, Schwaninger M and Koistinaho J: Nuclear factor-kappaB contributes to infarction after permanent focal ischemia. Stroke 35: 987-991, 2004.